New Journal of Physics
The open access journal at the forefront of physics

Deutsche Physikalische Gesellschaft DPG
IOP Institute of Physics

Published in partnership with: Deutsche Physikalische Gesellschaft and the Institute of Physics

OPEN ACCESS

RECEIVED
22 December 2020

REVISED
14 March 2021

ACCEPTED FOR PUBLICATION
18 March 2021

PUBLISHED
27 April 2021

PAPER

On the triad transfer analysis of plasma turbulence: symmetrization, coarse graining, and directional representation

S Maeyama[1,*], M Sasaki[2,3,4,5], K Fujii[6], T Kobayashi[7], R O Dendy[3,4,8], Y Kawachi[9], H Arakawa[10] and S Inagaki[2,3]

[1] Department of Physics, Nagoya University, Nagoya 464-8602, Japan
[2] Research Institute for Applied Mechanics, Kyushu University, Kasuga 816-8580, Japan
[3] Research Center for Plasma Turbulence, Kyushu University, Kasuga 816-8580, Japan
[4] Centre for Fusion, Space and Astrophysics, Department of Physics, Warwick University, Coventry CV4 7AL, United Kingdom
[5] College of Industrial Technology, Nihon University, Narashino, Chiba 275-8575, Japan
[6] Department of Mechanical Engineering and Science, Graduate School of Engineering, Kyoto University, Kyoto 615-8540, Japan
[7] National Institute for Fusion Science, Toki 509-5292, Japan
[8] CCFE, Culham Science Centre, Abingdon, Oxfordshire OX14 3DB, United Kingdom
[9] Interdisciplinary Graduate School of Engineering Sciences, Kyushu University, Kasuga 816-8580, Japan
[10] Institute of Science and Engineering, Academic Assembly, Shimane University, Matsue 690-8504, Japan
[*] Author to whom any correspondence should be addressed.

E-mail: smaeyama@p.phys.nagoya-u.ac.jp

Keywords: plasma turbulence, nonlinear transfer, triad interaction, network graph

Abstract

This article discusses triad transfer analysis via quadratic nonlinearity. To avoid fictitious interactions, symmetrization of the triad transfer is reviewed, including arbitrary orthogonal decomposition and coarse graining. The directional representation of the symmetrized triad transfer is proposed by minimizing the number of edges in a network graph of triad interactions with keeping the energy consistency. The directional representation simplifies visualization and allows us to reduce the energy transfer into a one-to-one relation, while eliminating fictitious interactions in non-symmetrized triad transfer functions. Energy transfer processes among plasma turbulent fluctuations that decompose by the singular value decomposition are analyzed as an application. A network graph visualization clearly demonstrates the importance of symmetrization and the consistency between the symmetrized triad transfer and its directional representation.

1. Introduction

Magnetically confined plasma is a non-equilibrium open system. It inherently contains micro-instabilities, dissipation, turbulence, and self-organized structures. The understanding of turbulent interactions among waves and vortices is great interest to plasma turbulence studies. Similar to the nonlinear advection term $\boldsymbol{v}\cdot\nabla\boldsymbol{v}$ in neutral fluid turbulence, electromagnetic nonlinearity in plasma turbulence is often quadratic. When attempting to distinguish typical waves and decompose the scales of vortices by an orthogonal decomposition $\boldsymbol{v}=\sum_k \boldsymbol{v}_k$ (e.g., via the Fourier transform), the energy transfer via the quadratic nonlinearity is described by triad interactions among three modes, namely k, p, and q.

Early studies of neutral fluid turbulence show that, in the symmetry of triad interactions, mode k is always simultaneously affected by a pair (p, q) and its permuted pair (q, p) [1]. Let $S_k^{p,q}=S_k^{q,p}$ be the symmetric triad transfer, which means that the energy transfers to the mode k via coupling with p and q. When considering isotropic turbulence, the shell-to-shell transfer function is often discussed by taking an angle average in Fourier wavenumber space while retaining the symmetric property among the three shells K, P, and Q, i.e., $S_K^{P,Q}=\sum_{k\in K}\sum_{p\in P}\sum_{q\in Q}S_k^{p,q}$ [2–4]. Besides the symmetric transfer are useful to analyze the wave–wave interactions, the non-symmetrized transfer functions are also adopted to analyze wave–mean flow interactions [5]. Some studies introduce a summation over an index of triad interactions to avoid the difficulty of visualizing triple indices (i.e., $S_K^Q=\sum_P S_K^{P,Q}$) [6], while it destroys the symmetric property. The development of diagnostic techniques of triad interactions is ongoing. For example, a recent paper discusses

a way to determine the energy flux vector of anisotropic turbulence in wavenumber space using the Moore–Penrose inverse [7], based on the locality of the net energy transfer [8, 9].

In a study of magnetohydrodynamic (MHD) turbulence, a non-symmetric energy transfer that satisfies the conservation between two modes is proposed to represent a mode-to-mode energy transfer [10]. Here, a non-symmetric energy transfer from q to k as $A_k^{p,q}$ is denoted, where the other mode of the triplet p is regarded as a mediator. Taking the shell average of this non-symmetric transfer and summation over the mediator ($A_K^Q = \sum_{k\in K}\sum_p\sum_{q\in Q}A_k^{p,q}$), the non-symmetric shell-to-shell transfer between the two shells K and Q has been extensively used for the analysis of MHD turbulence [11–15]. A similar formulation of non-symmetric transfer was applied in the analysis of microscopic turbulence in magnetized plasma [16–18]. Turbulent energy cascade has also been analyzed by a non-symmetric shell-to-shell transfer function of the gyrokinetic equation [19–21]. Recent studies use a non-symmetric shell-to-shell transfer for the analysis of multi-scale interactions [22], and discuss formulations based on a non-symmetric transfer function [23].

A possible disadvantage of the use of non-symmetrized transfer is that the choice of a function form of non-symmetrized transfer is not unique; it could contain fictitious interactions (as discussed in section 2.4). Symmetrization reviewed in this work is a procedure that extracts net energy gain and loss from the non-symmetrized transfer, so it should be unique. The importance of symmetrization was carefully pointed out by reference [24] in the context of gyrokinetic simulation studies of plasma turbulence: energy transfer from large to small scales via coupling with zonal flows can be evaluated by directly analyzing the symmetrized triad transfer function. Based on symmetrized triad transfer functions, cross-scale interactions are analyzed via symmetric subspace transfer functions [25], which are an extension of symmetric shell-to-shell transfer analyses, applicable for the anisotropic spectrum of plasma turbulence.

The discussion on the symmetrization of triad interactions is not limited to the Fourier basis. This consistently happens when fluctuations are decomposed into more than three components and interact, because of the arbitrariness of energy circulation among three components. In this paper, the energy transfer is analyzed with the aid of the singular value decomposition (SVD) or the proper orthogonal decomposition [26, 27]. The importance of symmetrization in gaining physical interpretation is also discussed. Although not performed here, the symmetrization of triad interactions could also be applied in bi-spectrum and bi-coherence analyses of three waves in frequency space. This is widely used in research on magnetic fusion [28–31] and space [32, 33] plasmas, the weak turbulence of gravity capillary waves [34], and in galaxy redshift analysis [35].

After evaluating the symmetrized triad transfer functions, there may be difficulty in analysis and visualization due to a large degree of freedom $S_k^{p,q}$. One way to solve this is through coarse graining (e.g., evaluation of shell-to-shell transfer or energy flux through a given cutoff [4]), although the dimension of $S_K^{P,Q}$ is still high. The next attempt to ease this difficulty is to take various slices by specifying one of the indices [3, 24], while it would be still difficult to take the whole picture into account. Because of the symmetry of $S_k^{p,q}$, the direction of energy transfer is not determined until the detailed balance among the triplet is checked. Another way to resolve the difficulty in visualization and analysis of triad interactions is to use a network graph that represents both the direction and the amplitude of the triad coupling.

The reminder of this paper is organized as follows. In section 2, energy transfer functions via quadratic nonlinearity are formulated. After non-symmetric transfer and its symmetrization are reviewed, directional representation of symmetrized transfer to represent the transfer processes by one-to-one relations is also discussed. In section 3, the non-symmetrized and symmetrized transfer functions are applied for the analysis of plasma turbulence simulation data decomposed by SVD. Network graph visualizations elucidate fictitious interactions in non-symmetrized transfer and the similarity between symmetrized triad transfer and its directional representation. Concluding remarks are given in section 4.

2. Analysis of energy transfer via quadratic nonlinearity

In this section, energy transfer functions are formulated and their directional representations are newly proposed. Although the energy transfer in turbulence is often analyzed with Fourier decomposition, the formulation is valid for any orthogonal decomposition. In order to explicitly show the general applicability of our discussion to any systems with quadratic nonlinearity, a model equation with an abstracted form is utilized here. A particular form for the vorticity equation with SVD appears later section 3.

2.1. Model equation

The turbulent fluctuations $f(t,\boldsymbol{x})$ are governed by the system below,

$$\frac{\partial f}{\partial t} = \{\phi, f\} + L, \tag{1}$$

where L denotes a linear term. The quadratic nonlinearity is described here by the Poisson brackets $\{\phi,f\} = -(\partial_x\phi\partial_y f - \partial_y\phi\partial_x f)$. This satisfies the first and second conservation properties $\int\{\phi,f\}\mathrm{d}\boldsymbol{x} = 0$ and $\int f\{\phi,f\}\mathrm{d}\boldsymbol{x} = \int \phi\{\phi,f\}\mathrm{d}\boldsymbol{x} = 0$ under the whole volume integral $\int\cdot\mathrm{d}\boldsymbol{x}$ and appropriate boundary conditions. Thus, the nonlinear term conserves squared quantities (e.g., $E = \frac{1}{2}\int f^2\,\mathrm{d}\boldsymbol{x}$) that hereafter refer to the total energy.

The above class of nonlinearity often appears to describe magnetized plasma turbulence that has quasi-two-dimensional properties originating from confinement magnetic field. For example, in electrostatic gyrokinetic equations [36], f is the plasma distribution function in the gyrocenter phase space $\boldsymbol{x} = (\boldsymbol{X},\boldsymbol{v})$ and ϕ is the gyrophase-averaged electrostatic potential. Thus, the nonlinear term describes the advection term by $E\times B$ flows $(-\nabla\phi\times\boldsymbol{z})/B_0\cdot\nabla f = (1/B_0)(\partial_x\phi\partial_y f - \partial_y\phi\partial_x f)$ under a homogeneous magnetic field $\boldsymbol{B}_0 = B_0\boldsymbol{z}$. In reduced MHD [37], the parallel electric field under the perturbed vector potential $\tilde{A}_\parallel$ is treated with $-\tilde{\boldsymbol{B}}_\perp\cdot\nabla_\perp\phi/B_0 = \boldsymbol{z}\times\nabla_\perp\tilde{A}_\parallel\cdot\nabla\phi/B_0 = (1/B_0)(\partial_x\tilde{A}_\parallel\partial_y\phi - \partial_y\tilde{A}_\parallel\partial_x\phi)$. In the Hasegawa–Watakani equation [38] or the Charney–Hasegawa–Mima equation [39, 40] of drift wave turbulence, f is the vorticity $f = \nabla^2\phi$ or the potential vorticity $f = \nabla^2\phi - \phi$.

The Navier–Stokes equation or the MHD equation might be considered to deal with the nonlinear terms like $\boldsymbol{v}\cdot\nabla\boldsymbol{v}$, $\boldsymbol{v}\cdot\nabla\boldsymbol{B}$, and $\boldsymbol{B}\cdot\nabla\boldsymbol{B}$ in three-dimensional problems. Because they are also quadratic nonlinearities satisfying conservation of squared quantities, the following discussion on symmetrization, coarse graining, and directional representation is applicable to them in the same way.

2.2. Decomposition of fluctuations

When we use the term 'interactions,' the existence of some modes (or waves, structures, and components) are implicit, all of which play important roles in describing the phenomena of interest. Then, an attempt is made to distinguish these modes by decomposing fluctuations,

$$f(t,\boldsymbol{x}) = \sum_k f_k(t,\boldsymbol{x}), \tag{2}$$

with any kind of transformation $f_k(t,\boldsymbol{x}) = \mathcal{F}_k[f(t,\boldsymbol{x})]$. The potential is also expanded as $\phi(t,\boldsymbol{x}) = \sum_k \phi_k(t,\boldsymbol{x})$, where each ϕ_k is associated with f_k. The summation of k is taken over all degrees of freedom. It is also desired that this decomposition satisfies the orthogonality, i.e., $\int f_k f_p\,\mathrm{d}\boldsymbol{x} = 0$ when $k\neq p$, because it allows energy to be split into each modes,

$$E = \sum_k E_k, \tag{3}$$

where $E_k = \frac{1}{2}\int |f_k|^2\,\mathrm{d}\boldsymbol{x}$ denotes the energy of each mode.

Under the decomposition, equation (1) is rewritten as

$$\sum_k \frac{\partial f_k}{\partial t} = \sum_p\sum_q \{\phi_p, f_q\} + L, \tag{4}$$

or, by applying the orthogonal transformation $\mathcal{F}_k$ on both the sides of the above equation, one yields the evolution equation of each mode,

$$\frac{\partial f_k}{\partial t} = \sum_p\sum_q M_k^{p,q}\phi_p f_q + L_k, \tag{5}$$

with a bi-linear coupling constant operator $M_k^{p,q} = \mathcal{F}_k[\{,\}]$ and $L_k = \mathcal{F}_k[L]$.

Hereafter, the contribution from the linear term L_k is suppressed to focus on interactions among modes through the nonlinear term. The effect of the linear term on the energy evolution equation should be analyzed separately. The linear term may provide driving sources of instabilities, dissipations by diffusion, collision, or wave–particle resonance damping, and linear mode coupling through background inhomogeneity. The linear term affects the properties of fluctuations, therefore altering the realization of nonlinear energy transfer processes. The methodology for nonlinear energy transfer diagnostics, presented in this paper, is applicable in analyzing the effects of multi-scale/multiple-type dissipation of the energy cascade [41–44].

2.3. Triad energy transfer functions

Multiplying f_k on equation (4) and integrating over the volume, one obtains the energy evolution equation for each mode,

$$\frac{\partial E_k}{\partial t} = T_k, \tag{6}$$

where the total energy transfer to the mode k is

$$T_k = \sum_p \sum_q A_k^{p,q}, \tag{7}$$

and satisfies $\sum_k T_k = 0$ from the second conservation property. The non-symmetrized triad transfer among modes k, p and q is given by

$$A_k^{p,q} = \int f_k \{\phi_p, f_q\} \mathrm{d}\boldsymbol{x}. \tag{8}$$

From equation (8), $A_k^{p,q} = -A_q^{p,k}$ is confirmed, pointing out the basis of non-symmetrized transfer between two modes k and q [10]. Although this definition appears straightforward, its usage for the analysis of triad interactions is not recommended, because it could contain fictitious interactions (discussed in a later section).

Because the dummy indices of summation, p and q, run over all degrees of freedom, a pair (e.g., $p = a, q = b$) and its permuted pair ($p = b, q = a$) are always included in equation (7). Thus, if the non-symmetrized triad transfer is split into symmetric and anti-symmetric parts with respect to p and q as $A_k^{p,q} = \frac{1}{2}(A_k^{p,q} + A_k^{q,p}) + \frac{1}{2}(A_k^{p,q} - A_k^{q,p})$, the latter part vanishes in the summation over the permuted pairs. Hence, the symmetric part is only able to contribute

$$T_k = \sum_p \sum_q S_k^{p,q}, \tag{9}$$

where the symmetrized triad transfer among modes k, p, q is defined by

$$S_k^{p,q} = \frac{1}{2}(A_k^{p,q} + A_k^{q,p}), \tag{10}$$

$$= \frac{1}{2} \int f_k \left[\{\phi_p, f_q\} + \{\phi_q, f_p\}\right] \mathrm{d}\boldsymbol{x}, \tag{11}$$

which trivially satisfies the symmetry for p and q, i.e., $S_k^{p,q} = S_k^{q,p}$. It also satisfies the detailed balance,

$$S_k^{p,q} + S_p^{q,k} + S_q^{k,p} = 0, \tag{12}$$

that corresponds to the energy conservation under the interaction among the triplet coupling k, p, and q.

2.4. Difference between non-symmetrized and symmetrized transfer

Figure 1 illustrates the energy transfer in a triad coupling. The symmetrized transfer denotes the net energy gain/loss of mode k via the coupling with the other modes p and q. This is expressed as $S_k^{p,q} + S_k^{q,p} = 2S_k^{p,q}$. Because the net energy gain/loss is unique, it can be uniquely constructed as $S_k^{p,q} = \frac{1}{2}(A_k^{p,q} + A_k^{q,p})$ from any expression of $A_k^{p,q}$. It is also clearly illustrated that the detailed balance, equation (12), corresponds to the energy conservation among k, p and q. In figure 1(a), the mode k gains the energy $S_k^{p,q} > 0$ via the triad coupling. Whether the origin is p or q cannot be identified only by observing $S_k^{p,q}$ because of the symmetry $S_k^{p,q} = S_k^{q,p}$. By checking the other components ($S_p^{q,k} < 0$, $S_q^{k,q} < 0$) and considering the detailed balance relation, it is concluded that energy is conservatively transferred from both of mode p and mode q to mode k. Thus, there is one taker and two givers in the case of figure 1(a).

Conversely, the non-symmetrized transfer analysis expresses the triad interactions as a set of one-to-one energy exchanges, as is shown in figure 1(b). Its basis is the anti-symmetric property $A_k^{p,q} = -A_q^{p,k}$, which ensures the energy conservation between k and q and therefore the other mode p is interpreted as a mediator. The net energy transfer to mode k via the coupling with p and q is given by $A_k^{p,q} + A_k^{q,p}$. This is consistent with the symmetrized transfer function $2S_k^{p,q}$. However, the definition of the non-symmetrized transfer, like equation (8), cannot be uniquely determined. As an example, in the Charney–Hasegawa–Mima equation, the nonlinear Poisson brackets can be equivalently expressed by the potential vorticity or the vorticity $\{\phi, \nabla^2\phi - \phi\} = \{\phi, \nabla^2\phi\}$, whereas the value of the non-symmetrized transfer $A_k^{p,q}$ can depend on the choice of a specific function form. See appendix A for details. The non-uniqueness of the non-symmetrized transfer originates from the arbitrary energy circulation of the three modes, that does not contribute to net energy transfer.

To recognize the apparent difference between symmetrized and non-symmetrized transfer functions, consider the no physical interaction case, $f = \phi$ where the Poisson brackets vanish $\{\phi, f\} = \{\phi, \phi\} = 0$. Nothing should happen physically. Now, when the fluctuations are decomposed into three modes $\phi = \phi_k + \phi_p + \phi_q$, examine the transfer functions. Although the symmetrized transfer function trivially satisfies $S_k^{p,q} = \frac{1}{2}\int \phi_k(\{\phi_p, \phi_q\} + \{\phi_q, \phi_p\})\mathrm{d}\boldsymbol{x} = 0$, the non-symmetrized transfer $A_k^{p,q} = \int \phi_k \{\phi_p, \phi_q\} \mathrm{d}\boldsymbol{x}$ is

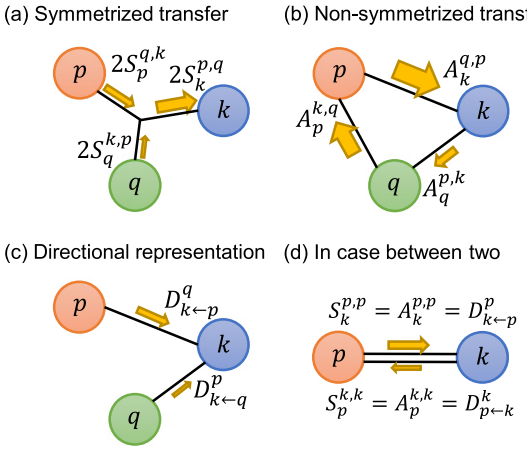

Figure 1. Schematic pictures of energy transfer among a triad coupling (k, p, and q) represented by (a) the symmetrized triad transfer function $S_k^{p,q}$, (b) the non-symmetrized triad transfer function $A_k^{p,q}$ (which satisfies $A_k^{p,q} = -A_q^{p,k}$), and (c) the directional representation $D_{k\leftarrow p}^q$. (d) Consistency of all definitions in the case of the interaction between two modes (i.e., two of triplet are the same). Widths and directions of the arrows represent the strength and sign of the transfer. For the symmetrized transfer, the arrow points toward the mode k when $S_k^{p,q} > 0$, while the arrow points away from k when $S_k^{p,q} < 0$. For the non-symmetrized transfer, the arrow points from q to k when $A_k^{p,q} > 0$, while opposite when $A_k^{p,q} < 0$. $D_{k\leftarrow q}^p$ is also similar to $A_k^{p,q}$.

generally non-vanishing. Hence, in the analysis based on the non-symmetrized triad transfer function, fictitious interactions could be observed because arbitrary circulations among the three modes can appear in the analysis. To avoid misinterpretation caused by fictitious interactions, the symmetrized triad transfer function is recommended, as it is uniquely determined as a net energy gain/loss.

2.5. Directional representation of the symmetrized transfer

The main motivation for the use of the non-symmetrized transfer is the simplification of visualization that can be obtained by expressing the triad transfer process as a one-to-one relation. For this purpose, the directional representation $D_{k\leftarrow q}^p$ is proposed. It is constructed from symmetrized triad transfer functions per the following rules:

- Anti-symmetry (conservation law between $k \leftrightarrow q$ via a mediator p):

$$D_{k\leftarrow q}^p = -D_{q\leftarrow k}^p. \tag{13}$$

- Consistency with symmetrized triad transfer as a net energy gain/loss:

$$S_k^{p,q} = \frac{1}{2}(D_{k\leftarrow q}^p + D_{k\leftarrow p}^q). \tag{14}$$

- No simultaneous gain and loss to a mode (minimizing the number of edges in a network graph of triad interactions):

$$D_{k\leftarrow q}^p = 0. \ \left[\text{if } \operatorname{sgn}(S_k^{p,q}) = \operatorname{sgn}(S_q^{k,p})\right]. \tag{15}$$

These conditions are valid for all permutations of k, p, and q. The first two are the same as the requirements of the non-symmetrized mode-to-mode transfer $A_k^{p,q}$. The first condition, equation (13), reduces the six unknown $D_{k\leftarrow q}^p$ to three. Three equations from the second condition, equation (14), are not enough to determine the unique $D_{k\leftarrow q}^p$ because of arbitrary circulation. This is the reason why the non-symmetrized mode-to-mode transfer $A_k^{p,q}$ cannot be uniquely constructed from the symmetrized transfer $S_k^{p,q}$. Any possibility of energy transfer between two modes cannot be rule out only by the energetic consistency. In this sense, the directional representation $D_{k\leftarrow q}^p$ is a special choice of non-symmetrized mode-to-mode transfer functions.

The third condition, equation (15), was introduced because of the following consideration: because of the detailed balance of the symmetrized triad transfer, $S_k^{p,q} + S_p^{q,k} + S_q^{k,p} = 0$, their possible sign combinations can be $(\operatorname{sgn}(S_k^{p,q}), \operatorname{sgn}(S_p^{q,k}), \operatorname{sgn}(S_q^{k,p})) = (-,-,+), (-,+,-)$, or $(+,-,-)$. Namely, there are two givers and one taker. The sign combinations can also be $(\operatorname{sgn}(S_k^{p,q}), \operatorname{sgn}(S_p^{q,k}), \operatorname{sgn}(S_q^{k,p})) = (-,+,+)$, $(+,+,-)$, or $(+,-,+)$. Namely, there is one giver and two takers [3]. What the symmetrized transfer function in figure 1(a) demonstrates is the net energy transfer to a mode under a triad coupling. Thus, to define a directional representation from the symmetrized transfer, it is natural to avoid a mode's simultaneous gain and loss. The third condition, equation (15), assures that givers should only give and

takers should only take. It can also be regarded as a minimization of the L1 norm $|D^p_{k\leftarrow q}| + |D^q_{p\leftarrow k}| + |D^k_{q\leftarrow p}|$. Because the condition $\mathrm{sgn}(S^{p,q}_k) = \mathrm{sgn}(S^{k,p}_q)$ means that both k and q are either givers or takers, equation (15) suppresses the energy transfer between two givers (or takers) in the directional representation, as is depicted in figure 1(c). Thus, in a network graph, the directional representation omits a network loop in triad interaction and minimizes the number of edges in the network. This is not merely simplification of visualization but a physical consideration. Even if there are simultaneous gains and losses to a mode, they should partially cancel out, and only the residual has physical contributions to the net energy transfer.

Another possible advantage of the directional representation is the analysis of the energy flux vector of anisotropic turbulence in wavenumber space. Because the directional representation expresses triad interactions as mode-to-mode energy transfer, its network visualization in wavenumber space represents the path of energy transfer independent of the locality assumption [7], while eliminating fictitious interactions arising from non-symmetrized transfer functions. This is also a useful feature in analyzing the energy transfer paths in the phase space of plasma turbulence [45]. The investigation of this fundamental aspect of plasma turbulence has increased, and will likely be a new Frontier in turbulence research. See the publications about gyrokinetics [46, 47], hybrid gyrokinetics (gyrokinetic ions and fluid electrons) [48] and hybrid kinetics (fully kinetic ions and fluid electrons) [49] for more details.

2.6. Procedures for symmetrization and directional representation

The procedure for triad transfer analysis is summarized below.

(a) Formulate the equation of the energy for each mode as equation (6) and indicate at least one expression of the non-symmetrized triad transfer function $A^{p,q}_k$. It should satisfy the total energy consistency, equation (7), although an anti-symmetric property such as $A^{p,q}_k = -A^{p,k}_q$ is not necessarily required ($A^{p,q}_k$ is not directly analyzed as a one-to-one energy transfer).

(b) Symmetrize the transfer by equation (10), which uniquely defines the symmetrized transfer $S^{p,q}_k$ from any $A^{p,q}_k$. The total energy consistency, equation (9), and the detailed balance, equation (12), should be confirmed. Analyze triad interactions based on the symmetrized transfer. Some examples of plots are found in references [3, 4, 24, 25].

(c) Construct the directional representation $D^p_{k\leftarrow q}$ from the symmetrized triad transfer function as defined in equations (13)–(15). This may help with the analysis and visualization of the symmetrized transfer.

Because the last step is represented by more than just algebraic expressions, the construction of the directional representation from an example in figures 1(a) and (c) is examined. As both p and q are givers, the third condition imposed by equation (15) is $D^k_{p\leftarrow q} = D^k_{q\leftarrow p} = 0$. Then, from the second condition equation (14), $D^q_{p\leftarrow k} = 2S^{q,k}_p$ and $D^p_{q\leftarrow k} = 2S^{k,p}_q$. Finally, equation (13) gives $D^p_{k\leftarrow q} = -D^p_{q\leftarrow k}$ and $D^q_{k\leftarrow p} = -D^q_{p\leftarrow k}$.

Figures 1(a)–(c) explains the case of three independent modes (k, p, q). Figure 1(d) shows the case where two modes in the triplet are the same, e.g., (k, p, p) and (k, k, p). Even in this case, the definitions of equations (6)–(15) are valid. The yield is $S^{p,p}_k = A^{p,p}_k = D^p_{k\leftarrow p} (= -2S^{k,p}_p = -A^{p,k}_p = -D^p_{p\leftarrow k})$ for (k, p, p). The yield of (k, k, p) is similar. Because the interactions are between two modes k and p, circulation among three modes does not appear, so all the definitions of triad transfer functions are consistent. In the case where the triplet is of a single mode (k, k, k), $S^{k,k}_k = A^{k,k}_k = D^k_{k\leftarrow k} = 0$ trivially vanishes.

So far, the case of $S^{p,q}_k = 0$ in the definition of the directional representation has been excluded. When one of the symmetrized transfer functions vanishes (e.g., the mode p has no gain/loss so $S^{q,k}_p = 0$), the detailed balance becomes $S^{p,q}_k = -S^{k,p}_q$ meaning the energy transfers from q to k or vice versa. Per the rule of no simultaneous gain and loss to a mode, the directional transfer is naturally defined as $D^p_{k\leftarrow q} = 2S^{p,q}_k$ and $D^q_{p\leftarrow k} = D^k_{q\leftarrow p} = 0$. To apply equation (15) technically, first, assume $S^{q,k}_p = +\varepsilon$ and take the limit of $\varepsilon \to 0$. Then, $D^q_{p\leftarrow k} + D^k_{p\leftarrow q} = 0$ from equation (14), and one of them is zero from equation (15), then $D^q_{p\leftarrow k} = D^k_{q\to p} = 0$.

2.7. Coarse graining by summarizing modes

In section 2.2, an orthogonal decomposition of fluctuations was the starting point of the discussion of triad energy transfer. Coarse graining of fluctuations by taking shell averages of Fourier transform as $f_K = \sum_{k\in K} f_k$ with $f_k = \hat{f}_k(t)\exp(\mathrm{i}\boldsymbol{k}_k\cdot\boldsymbol{x}) + \mathrm{c.c.}$ are also regarded as orthogonal decompositions. $\int f_K f_P \,\mathrm{d}\boldsymbol{x} = 0$, when shells $K = \{k_K - \Delta/2 < |\boldsymbol{k}| < k_K + \Delta/2\}$ and $P = \{k_P - \Delta/2 < |\boldsymbol{k}| < k_P + \Delta/2\}$ have no intersection [3]. k_K and Δ denote the centered wavenumber and the width of the shell, respectively. Similarly, the arbitrary subspace of wavenumber space (rather than isotropic shells) is defined as $f_{\Omega_K} = \sum_{k\in\Omega_K} f_k$, without intersections $\int f_{\Omega_K} f_{\Omega_P}\,\mathrm{d}\boldsymbol{x} = 0$, allowing more flexible analysis of anisotropic or

scale-separated turbulence in magnetized plasmas [25]. Coarse graining to SVD may also be applied by summarizing some modes depending on their features.

Coarse graining of the triad transfer function can be constructed from fine transfer,

$$S_{\Omega_K}^{\Omega_P,\Omega_Q} = \sum_{k\in\Omega_K}\sum_{p\in\Omega_P}\sum_{q\in\Omega_Q} S_k^{p,q}. \tag{16}$$

but it would be numerically less efficient. As the coarse decomposition $f = \sum_{\Omega_K} f_{\Omega_K}$ is also an orthogonal decomposition, the procedures from equations (6)–(15) can be applied directly to f_{Ω_K}, where the degree of freedom Ω_K is significantly reduced from that of the fine decomposition k.

There is a different type of coarse graining that can be utilized by applying space filtering (that does not necessarily construct orthogonal decomposition). Filtering of configuration space and velocity space has become a recent interest in kinetic plasma turbulence studies [50–52].

3. Application examples

3.1. Evaluation of energy transfer in plasma turbulence by SVD

Here, the energy transfer process during limit-cycle oscillation (LCO) is analyzed, as it is observed in the plasma turbulence simulation of reference [53]. Under the homogeneous magnetic fields $\boldsymbol{B}_0 = B_0\boldsymbol{z}$, the time evolution of global fluid dynamics of cylindrical plasma is described through fluid equations based on the Hasegawa–Wakatani model [54]. A radially inhomogeneous background flow is applied by a vorticity source, and this velocity inhomogeneity excites the Kelvin–Helmholtz instability. When the source is above a certain intensity level and there is a growth in the Kelvin–Helmholtz instability, an abrupt formation of zonal flows accompanying spiral flow structures, relaxing background flows, and the disappearance of fluctuating flow patterns occurs repeatedly, exhibiting the LCO.

Because the electrostatic potential ϕ represents the stream function of the $E\times B$ flow $\boldsymbol{v} = \boldsymbol{z}\times\nabla\phi/B_0$, typical spatial structures of the flow are obtained from SVD on the potential distribution,

$$\phi(r,\theta,t) = \sum_j s_j\Psi_j(r,\theta)h_j(t), \tag{17}$$

where Ψ_j, h_j, and s_j, respectively, describe the spatial mode pattern, the temporal evolution of amplitude, and the singular value, respectively, of the jth mode corresponding to its relative contribution to the whole data $\phi(r,\theta,t)$. The orthogonality condition $\int \phi_i(r,\theta)\phi_j(r,\theta)r\,\mathrm{d}r\,\mathrm{d}\theta = 0$ when $i\neq j$ carries the cylindrical Jacobian r, so it remains consistent with a physical kinetic energy evaluation. Some pairs of SVD modes have singular values with nearly the same amplitudes. In combination, these modes represent azimuthal propagation, akin to sine and cosine in the Fourier mode decomposition. Thus, reference [53] decomposes electrostatic potential fluctuations into four dominant modes after taking a summation of some pairs,

$$\phi(r,\theta,t) = \sum_{k=A,B,C,D}\phi_k(r,\theta,t). \tag{18}$$

Figure 2, reproduced from reference [53], shows the spatial flow patterns and their physical interpretations are as follows. Mode A corresponds to the background flow inhomogeneity induced by the vorticity source. Mode B represents the azimuthally symmetric zonal flow. Mode C is the Kelvin–Helmholtz mode destabilized by the background flow inhomogeneity. Mode D is the intermittent spiral structure that appears during an LCO event.

3.2. Triad energy transfer based on vorticity equation

The energy transfer among the SVD modes is analyzed based on the vorticity equation

$$\frac{\partial\nabla^2\phi}{\partial t} = -\{\phi,\nabla^2\phi\} + L, \tag{19}$$

where on the right-hand side the first term $\{\phi,\nabla^2\phi\} = (1/r)(\partial_r\phi\partial_\theta\nabla^2\phi - \partial_\theta\phi\partial_r\nabla^2\phi)$ represents the nonlinear convective derivative of the $E\times B$ flow, and the second term L contains a collisional dissipation and the vorticity source. The kinetic energy equation of each mode ($k = A, B, C, D$) is obtained by multiplying ϕ_k and taking the spatial integral,

$$\frac{\partial E_k}{\partial t} = T_k - \int \phi_k L r\,\mathrm{d}r\,\mathrm{d}\theta, \tag{20}$$

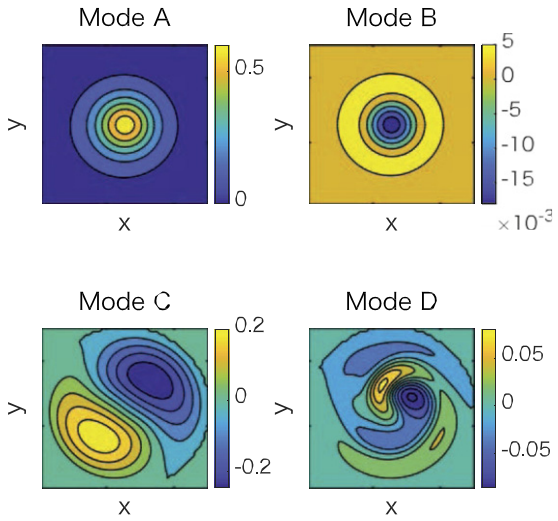

Figure 2. Spatial flow patterns extracted by applying SVD on the electrostatic potential. Modes *A*, *B*, *C* and *D* denote the background flow inhomogeneity, zonal flows, Kelvin–Helmholtz mode, and intermittent spiral structures, respectively. Reprinted from reference [53] with permission of IOP Publishing.

where the energy of each mode is defined by $E_k = \frac{1}{2}\int |\nabla\phi_k|^2 r\,\mathrm{d}r\,\mathrm{d}\theta$. The total energy transfer to a mode T_k is represented by the summation of either the non-symmetrized $A_k^{p,q}$ or symmetrized $S_k^{p,q} = \frac{1}{2}(A_k^{p,q} + A_k^{q,p})$ energy transfer among triplet k, p, and q,

$$T_k = \sum_p\sum_q A_k^{p,q} = \sum_p\sum_q S_k^{p,q}, \tag{21}$$

$$A_k^{p,q} = \int \phi_k\{\phi_p, \nabla^2\phi_q\} r\,\mathrm{d}r\,\mathrm{d}\theta, \tag{22}$$

$$S_k^{p,q} = \frac{1}{2}\int \phi_k\left[\{\phi_p, \nabla^2\phi_q\} + \{\phi_q, \nabla^2\phi_p\}\right] r\,\mathrm{d}r\,\mathrm{d}\theta, \tag{23}$$

where the summation indices p and q run from A to D. From the property $A_k^{p,q} = -A_p^{k,q}$, $A_k^{p,q}$ can be referred to as the non-symmetrized mode-to-mode transfer from p to k via the coupling with a mediator q. The directional representation $D^p_{k\leftarrow q}$ can also be constructed from the symmetrized transfer $S_k^{p,q}$ as was described in section 2.5.

Figure 3(a), reproduced from reference [53], shows the time evolution of kinetic energy of a typical LCO event. After the development of background flow inhomogeneity (mode *A*), the coherent Kelvin–Helmholtz mode (mode *C*) is destabilized. Around $t = 60$, the growth of the Kelvin–Helmholtz mode saturates and the background flow inhomogeneity is reduced. Intermittent spiral structures (mode *D*) and zonal flows (mode *B*) subsequently develop. Figures 3(b)–(f) plots the total and symmetrized triad energy transfers. The Kelvin–Helmholtz mode is initially excited by the background flow inhomogeneity $2S_C^{A,C} > 0$, and there is no coupling between *A* and *B* because they are both azimuthally homogeneous $\partial_\theta \sim 0$ so that the Poisson bracket vanishes. In principle, it is possible to read all energy transfer processes from the figure. Practically, however, this may be difficult for unfamiliar analysts because the directions of the triad interactions are determined by considering the detailed balance.

3.3. Analysis of the triad transfer with the aid of graph visualization

Triad interactions are naturally visualized in network graphs. A Python interface of Graphviz [55] is used in this research.

Network graphs of the symmetrized triad transfer $S_k^{p,q}$ and its directional representation $D^p_{k\leftarrow q}$ are shown in figures 4 (a)–(e) and (f)–(j), respectively. In the graph of the symmetrized transfer, the detailed balance $S_k^{p,q} + S_p^{q,k} + S_q^{k,p} = 0$ is satisfied in a triad coupling represented by a junction of the triplet (k, p, q). The paths of the energy transfer among the modes are identified through the junctions. The directional representation $D^p_{k\leftarrow q}$ plots paths naturally consistent with the ones that are observed in the symmetrized transfer function. For example, at $30 < t < 40$, the interactions between the two are the same ($2S_A^{C,C} = D^C_{A\leftarrow C}$). At $70 < t < 80$, the interaction among the triplet (B, C, D), where *B* is a giver and *C* and *D* are takers, is expressed so that *B* gives energy to *C* and *D*.

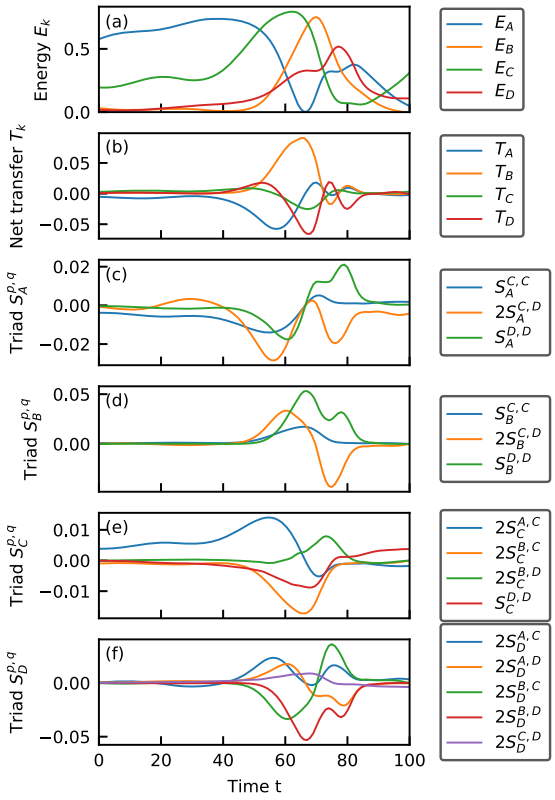

Figure 3. Time evolution at an LCO event. (a) Energy of each mode (*A*: background flow inhomogeneity, *B*: zonal flow, *C*: Kelvin–Helmholtz mode, *D*: intermittent spiral structure), (b) total energy transfer to a mode, (c)–(f) symmetrized triad energy transfer functions $S_k^{p,q}$. When the upper indices *p* and *q* are different, the net transfer is summarized as $S_k^{p,q} + S_k^{q,p} = 2S_k^{p,q}$. Panels (a) and (c)–(f) are identical to figure 7 Adapted from [53]. while small contributions less than ten percent of the maximum are omitted.

Figures 4(f)–(j) [or equivalently (a)–(e)] clearly shows the energy transfer processes during an LCO event. Early in the event, at $t < 50$, energy is transferred from the background flow inhomogeneity (mode *A*) to the Kelvin–Helmholtz mode (mode *C*). As the Kelvin–Helmholtz mode increases, intermittent spiral structures (mode *D*) are gradually excited. Its main path is $D^C_{D\leftarrow A} > 0$ at $50 < t < 60$. The Kelvin–Helmholtz mode *C* brings energy to the intermittent spiral structures in mode *D* while destroying the background flow inhomogeneity in mode *A*. After that, zonal flows (mode *B*) are generated, where energy transfers by coupling with the intermittent spiral structure ($D^C_{B\leftarrow D} > 0$ and $D^D_{B\leftarrow D} > 0$) dominate rather than being directly driven by the Kelvin–Helmholtz mode ($D^C_{B\leftarrow C} > 0$) as observed at $50 < t < 60$ and $60 < t < 70$. At $70 < t < 80$, the generated zonal flows (mode *B*) begin to decay into structures *C* and *D*. Because mode *C* also contains fine structures, it tends to facilitate the dissipation of total kinetic energy. The intermittent spiral structures play an important role in exciting zonal flows during an LCO event. The network graph visualization clearly demonstrates the validity of the symmetrized triad transfer function and its consistency with the directional representation.

The directional representation is naturally consistent with the transfer process observed in the symmetrized triad transfer function and simplifies its visualization. This is a powerful tool, especially when the number of modes *n* becomes large. In the symmetrized triad transfer function, the number of junctions representing a triplet [e.g., (k,p,q), (k,p,p), and (k,k,p)] is $m = \binom{n}{3} + 2\binom{n}{2}$. The total number of nodes is $n + m = \binom{n+2}{3}$. As a junction of three modes has three edges and a junction of two modes has an edge in each, the number of edges is $3\binom{n}{3} + 4\binom{n}{2} = (n+2)\binom{n}{2}$. Conversely, in the directional representation, the number of nodes is the same as the number of modes *n*. This is significantly reduced from the symmetrized transfer. Because one of the edges in a triad coupling with three modes is suppressed, as shown in figure 1(c), the number of edges is $2\binom{n}{3} + 2\binom{n}{2} = 2\binom{n+1}{3}$. This is reduced from the symmetrized transfer by a factor $\sim 2/3$.

The graph visualization also reveals the importance of symmetrization in avoiding fictitious interactions from the non-symmetrized transfer. From figures 4(k)–(o), impressions may be different from those of the symmetrized transfer. Additionally, the definition of $A_k^{p,q}$ is not unique. For example, a different definition $\tilde{A}_k^{p,q} = \int \phi_k\{\phi_p, \nabla^2\phi_q - \phi_q\} r\,\mathrm{d}r\,\mathrm{d}\theta$ also satisfies equation (21) and $A_k^{p,q} = -A_p^{k,q}$. Depending on the definition, figures 4(k)–(o) can be altered. These fictitious interactions could lead to incorrect physical

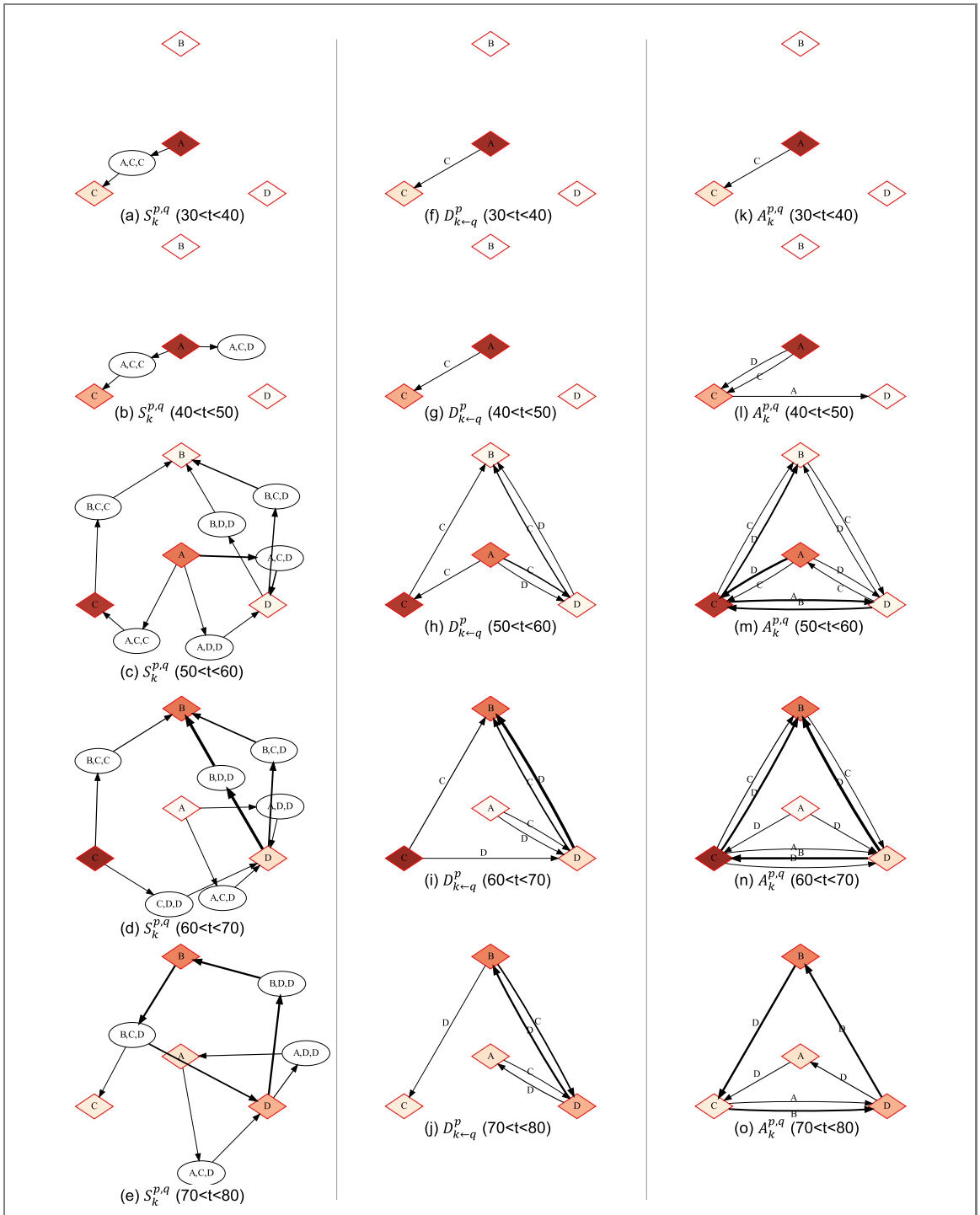

Figure 4. Graph visualization of triad transfer functions. Diamond nodes denote the modes of fluctuations (A–D) and their shading correspond to their kinetic energy. The energy transfer is represented by arrows, the widths of which represent the amplitude of the transfer. They are averaged during short periods from $30 < t < 40$ to $70 < t < 80$, and small transfers less than ten percent of the maximum are suppressed for visibility. Graphs (a)–(e) plot the symmetried transfer $S_k^{p,q}$, where circular nodes represent the triad coupling as a junction of corresponding triplet (k, p, q). Graphs (f)–(j) plot the directional representation $D_{k\leftarrow q}^{p}$, where characters accompanying with arrows denote the mode of the mediator. Graphs (k)–(o) plot the non-symmetrized transfer $A_k^{p,q}$.

interpretations. Despite the choice of specific non-symmetrized transfer function forms, the net energy gain/loss to a mode should be immutable. This is why diagnosing the symmetrized transfer is recommended.

The methodology considered in the non-symmetrized mode-to-mode transfer analysis could be replaced using directional representation, as it is uniquely constructed from the symmetrized transfer function and is regarded as mode-to-mode transfer via a mediator. Figure 5 plots the contracted

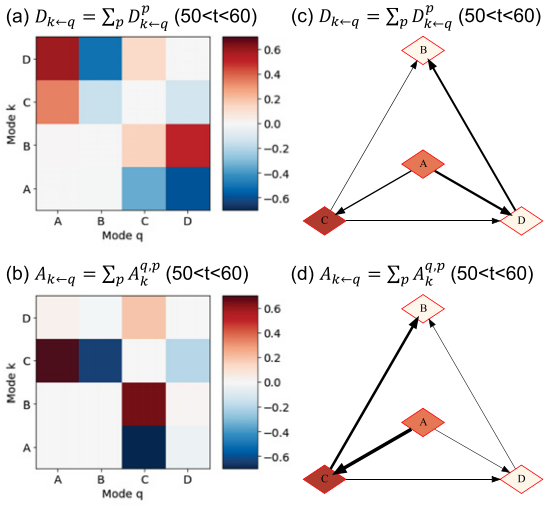

Figure 5. Mode-to-mode transfer from q to k contracted over the index of a mediator p based on (a) the directional representation $D_{k\leftarrow q} = \sum_p D^p_{k\leftarrow q}$ and on (b) the non-symmetrized triad transfer $A_{k\leftarrow q} = \sum_p A^{q,p}_k$ (which satisfies $A^{p,q}_k = -A^{k,q}_p$) at $50 < t < 60$. Positive values means the mode k obtains energy from mode p, and vice versa. Their graph visualization are also plotted in (c) and (d), respectively.

mode-to-mode transfer

$$D_{k\leftarrow q} = \sum_p D^p_{k\leftarrow q}, \tag{24}$$

that is regarded as the energy transfer from q to k summed over the index of the mediator p. The same transfer, defined using a non-symmetrized transfer, is also plotted for comparison. Because they describe simple one-to-one relations, they can be visualized by conventional two-dimensional images (a) and (b), as well as in the equivalent network graphs (c) and (d). (The question arises whether $\sum_p S^{p,q}_k$ would also be regarded as a mode-to-mode transfer from q to k. However, this quantity is nonsense. Generally, $\sum_p S^{p,k}_k \neq 0$, but an energy transfer from k to k should be 0. Because p and q are symmetric, the direction of transfer from the symmetrized function cannot be distinguished without examining the detailed balance).

The directional representation in figures 5(a) and (c) shows that the zonal flow B is excited mainly by the energy transfer from the intermittent spiral structure D, which is consistent with the observation in the symmetrized triad transfer in figure 4(c). Conversely, it can be seen from the non-symmetrized transfer function in figures 5(b) and (d) that the zonal flow seems to be excited only by the Kelvin–Helmholtz mode C. This obscures the importance of the intermittent spiral structure [53].

4. Summary

This paper discussed the triad transfer analysis techniques used to investigate interactions via quadratic nonlinearity in plasma turbulence. Directional representation of the symmetrized triad transfer function was developed to simplify visualization and to assist with analysis by expressing the transfer process as a one-to-one relation. It was uniquely defined by the conditions set out by equations (13)–(15), energetic consistency, and minimizing the number of edges in a network graph of triad interactions.

Section 2.6 summarizes the guidelines for triad transfer analysis. Any orthogonal decompositions and any coarse graining that keeps the orthogonality were applicable. The discussion on symmetrization was not limited to Fourier analysis. When triad interactions were considered, a non-symmetrized transfer function was not unique, as fictitious interactions can slip into the analysis because of the arbitrary circulation among the three modes. Symmetrization is a necessary procedure to evaluate the net energy gain/loss of a mode via the triad coupling.

Energy transfer processes, during LCOs in Hasegawa–Wakatani plasma turbulence, were analyzed. With the aid of the network graph visualization, the importance of the symmetrized triad transfer function and its consistency with directional representation was confirmed. By taking a summation of the directional representation over the index of a mediator, a mode-to-mode transfer analysis was reproduced, whereas fictitious interactions in non-symmetrized transfers were successfully omitted.

Throughout the paper, attentions was called to non-symmetrized transfer analysis, as it has been widely used in plasma research. Analysis based on symmetrized triad transfer functions is rigid and reliable.

Directional representation is also available for mode-to-mode transfer analysis as it is consistent with symmetrized transfer functions. Utilizing these energy transfer analyses with a correct understanding of their limitations will be helpful in exploration of plasma turbulence physics.

Acknowledgments

This work was partially supported by MEXT as 'Program for Promoting Researches on the Supercomputer Fugaku' (Exploration of burning plasma confinement physics), MEXT KAKENHI Grant Number JP20K03892, 'Joint Usage/Research Center for Interdisciplinary Large-scale Information Infrastructures' and 'High Performance Computing Infrastructure' (jh200053-MDHI), and the NIFS Collaboration Research Program (NIFS18KNWT001) in Japan. This work received support from the RCUK Energy Programme Grant No. EP/T012250/1. It was carried out within the framework of the EUROfusion Consortium and has received funding from the Euratom research and training programme 2014–2018 and 2019–2020 under Grant agreement No. 633053. The views and opinions expressed herein do not necessarily reflect those of the European Commission. The authors would like to thank Enago (www.enago.jp) for the English language review. Numerical analyses were performed on the supercomputer Flow at Nagoya University, the JFRS-1 at the Computational Simulation Centre of International Fusion Energy Research Centre (IFERC-CSC), and the Plasma simulator at the National Institute for Fusion Science.

Data availability statement

The data that support the findings of this study are openly available at the following URL/DOI: https://github.com/smaeyama/triadgraph. The computer code of the triad transfer analysis, the simulation data of the energy of SVD modes and non-symmetrized transfer are provided. The computer code contains a function to construct the symmetrized triad transfer from a non-symmetrized transfer, a function to construct the directional representation from the symmetrized triad transfer, and functions to draw network graphs of the symmetrized transfer and of the directional representation.

Appendix A. Example of the non-uniqueness of the non-symmetrized transfer

Depending on the ways to derive the energy equations, equations (6) and (7), non-symmetrized transfer functions would not necessarily be unique or antisymmetric. Considering the conservation laws in the Charney–Hasegawa–Mima equation will help understand this concept:

$$\frac{\partial(\nabla^2\phi-\phi)}{\partial t}=\{\phi,\nabla^2\phi\}, \tag{25}$$

where the linear terms are omitted. The quantity $f=\nabla^2\phi-\phi$ is the potential vorticity. By splitting the fluctuations $f=\sum_k f_k$ and multiplying f_k, the evolution equation of potential enstrophy of each mode $E_k=\frac{1}{2}\int|f_k|^2\,\mathrm{d}\boldsymbol{x}$ as $\frac{\mathrm{d}}{\mathrm{d}t}E_k=T_k$ is revealed. In the above heuristic derivation, a non-symmetrized transfer function $\breve{A}_k^{p,q}$ satisfying the total energy consistency $T_k=\sum_p\sum_q\breve{A}_k^{p,q}$ may be found as,

$$\breve{A}_k^{p,q}=\int f_k\{\phi_p,\nabla^2\phi_q\}\mathrm{d}\boldsymbol{x}. \tag{26}$$

Because this is not anti-symmetric $\breve{A}_k^{p,q}\neq\breve{A}_q^{p,k}\neq\breve{A}_p^{k,q}$, $\breve{A}_k^{p,q}$ cannot be recognized as a mode-to-mode transfer. The transfer is now symmetrized,

$$\begin{aligned}\breve{S}_k^{p,q}&=\frac{1}{2}(\breve{A}_k^{p,q}+\breve{A}_k^{q,p}),\\&=\int f_k[\{\phi_p,\nabla^2\phi_q\}+\{\phi_q,\nabla^2\phi_p\}]\mathrm{d}\boldsymbol{x},\\&=\int f_k[\{\phi_p,f_q\}+\{\phi_q,f_p\}]\mathrm{d}\boldsymbol{x},\end{aligned} \tag{27}$$

where $\{\phi_p,\phi_q\}+\{\phi_q,\phi_p\}=0$ is used at the last line. The total energy consistency $T_k=\sum_p\sum_q\breve{S}_k^{p,q}$ and the detailed balance $\breve{S}_k^{p,q}+\breve{S}_k^{p,q}+\breve{S}_k^{p,q}=0$ are confirmed.

The evolution equation can be derived in another way after rewriting the governing equation as $\partial_t f = \{\phi, f\}$ using $\{\phi, \phi\} = 0$. Following the same procedures, the non-symmetrized transfer $A_k^{p,q} = \int f_k \{\phi_p, f_q\} \mathrm{d}\boldsymbol{x}$ is obtained that possesses the anti-symmetric property. The symmetrized transfer is also constructed as $S_k^{p,q} = \frac{1}{2}(A_k^{p,q} + A_k^{q,p})$. Although the above two non-symmetrized transfer functions are not identical $\breve{A}_k^{p,q} \neq A_k^{p,q}$, the symmetrized transfer functions constructed by them are unchanged $\breve{S}_k^{p,q} = S_k^{p,q}$. This is because $S_k^{p,q}$ represents the net energy gain/loss, that corresponds to the physical excitation/suppression of the mode.

ORCID iDs

S Maeyama https://orcid.org/0000-0001-9338-0740
M Sasaki https://orcid.org/0000-0001-6835-1569
K Fujii https://orcid.org/0000-0003-0390-9984
T Kobayashi https://orcid.org/0000-0001-5669-1937
Y Kawachi https://orcid.org/0000-0002-5222-6082
H Arakawa https://orcid.org/0000-0001-9793-099X

References

[1] Kraichnan R H 1959 *J. Fluid Mech.* **5** 497
[2] Waleffe F 1992 *Phys. Fluids* A **4** 357
[3] Ohkitani K and Kida S 1992 *Phys. Fluids* A **4** 794
[4] Watanabe T and Iwayama T 2007 *Phys. Rev.* E **76** 046303
[5] Smyth W D 1992 *Phys. Fluids* A **4** 340
[6] Maltrud M E and Vallis G K 1993 *Phys. Fluids* A **5** 1760
[7] Yokoyama N and Takaoka M 2021 *J. Fluid Mech.* **908** A17
[8] Richardson L F and Lynch P 2007 *Weather Prediction by Numerical Process* 2nd edn (Cambridge: Cambridge University Press)
[9] Sharma M K, Verma M K and Chakraborty S 2019 *Phys. Fluids* **31** 085117
[10] Dar G, Verma M K and Eswaran V 2001 *Phys.* D **157** 207
[11] Alexakis A, Mininni P D and Pouquet A 2005 *Phys. Rev.* E **72** 046301
[12] Mininni P D, Alexakis A and Pouquet A 2005 *Phys. Rev.* E **72** 046302
[13] Mininni P D 2011 *Annu. Rev. Fluid Mech.* **43** 377
[14] Grete P, O'Shea B W, Beckwith K, Schmidt W and Christlieb A 2017 *Phys. Plasmas* **24** 092311
[15] Meyrand R, Kiyani K H, Gürcan Ö D and Galtier S 2018 *Phys. Rev.* X **8** 031066
[16] Holland C, Tynan G R, Fonck R J, McKee G R, Candy J and Waltz R E 2007 *Phys. Plasmas* **14** 056112
[17] Friedman B, Carter T A, Umansky M V, Schaffner D and Dudson B 2012 *Phys. Plasmas* **19** 102307
[18] Sasaki M, Kasuya N, Itoh K, Yagi M and Itoh S-I 2014 *Nucl. Fusion* **54** 114009
[19] Tatsuno T, Barnes M, Cowley S C, Dorland W, Howes G G, Numata R, Plunk G G and Schekochihin A A 2010 *J. Plasma Fusion Res. Series* **9** 509
[20] Plunk G G, Tatsuno T and Dorland W 2012 *New J. Phys.* **14** 103030
[21] Navarro A B, Teaca B, Jenko F, Hammett G W and Happel T (ASDEX Upgrade Team) 2014 *Phys. Plasmas* **21** 032304
[22] Howard N T, Holland C, White A E, Greenwald M and Candy J 2016 *Nucl. Fusion* **56** 014004
[23] Teaca B, Jenko F and Told D 2017 *New J. Phys.* **19** 045001
[24] Nakata M, Watanabe T-H and Sugama H 2012 *Phys. Plasmas* **19** 022303
[25] Maeyama S, Watanabe T-H, Idomura Y, Nakata M, Ishizawa A and Nunami M 2017 *Nucl. Fusion* **57** 066036
[26] Berkooz G, Holmes P and Lumley J L 1993 *Annu. Rev. Fluid Mech.* **25** 539
[27] Dudok T W, Pecquet A L, Vallet J C and Lima R 1994 *Phys. Plasmas* **1** 3288
[28] Kim Y C and Powers E J 1979 *IEEE Trans. Plasma Sci.* **7** 120
[29] Ritz C P *et al* 1988 *Rev. Sci. Instrum.* **59** 1739
[30] Itoh K, Nagashima Y, Itoh S-I, Diamond P H, Fujisawa A, Yagi M and Fukuyama A 2005 *Phys. Plasmas* **12** 102301
[31] Xu M *et al* (HL-2A Team) 2012 *Phys. Rev. Lett.* **108** 245001
[32] Lagoutte D, Lefeuvre F and Hanasz J 1989 *J. Geophys. Res.* **94** 435
[33] Henri P, Briand C, Mangeney A, Bale S D, Califano F, Goetz K and Kaiser M 2009 *J. Geophys. Res.* **114** A03013
[34] Aubourg Q and Mordant N 2015 *Phys. Rev. Lett.* **114** 144501
[35] Verde L *et al* 2002 *Mon. Not. R. Astron. Soc.* **335** 432
[36] Garbet X, Idomura Y, Villard L and Watanabe T H 2010 *Nucl. Fusion* **50** 043002
[37] Hazeltine R D and Meiss J D 2003 *Plasma Confinement* (New York: Dover)
[38] Hasegawa A and Wakatani M 1983 *Phys. Rev. Lett.* **50** 682
[39] Charney J G 1971 *J. Atmos. Sci.* **28** 1087
[40] Hasegawa A and Mima K 1977 *Phys. Rev. Lett.* **39** 205
[41] Bratanov V, Jenko F, Hatch D R and Wilczek M 2013 *Phys. Rev. Lett.* **111** 075001
[42] Cerri S S, Navarro A B, Jenko F and Told D 2014 *Phys. Plasmas* **21** 082305
[43] Told D, Jenko F, TenBarge J M, Howes G G and Hammett G W 2015 *Phys. Rev. Lett.* **115** 025003
[44] Passot T and Sulem P L 2015 *Astrophys. J.* **812** L37
[45] Meyrand R, Kanekar A, Dorland W and Schekochihin A A 2019 *Proc. Natl Acad. Sci. USA* **116** 1185
[46] Watanabe T-H and Sugama H 2004 *Phys. Plasmas* **11** 1476
[47] Hatch D R, Jenko F, Navarro A B and Bratanov V 2013 *Phys. Rev. Lett.* **111** 175001
[48] Kawazura Y, Barnes M and Schekochihin A A 2019 *Proc. Natl Acad. Sci. USA* **116** 771

[49] Cerri S S, Kunz M W and Califano F 2018 *Astrophys. J.* **856** L13
[50] Eyink G L 2018 *Phys. Rev.* X **8** 041020
[51] Cerri S S and Camporeale E 2020 *Phys. Plasmas* **27** 082102
[52] Teaca B, Gorbunov E, Told D, Navarro A B and Jenko F F 2021 *J. Plasma Phys.* **87** 905870209
[53] Sasaki M, Kobayashi T, Dendy R O, Kawachi Y, Arakawa H and Inagaki S 2020 *Plasma Phys. Control. Fusion* **63** 025004
[54] Sasaki M *et al* 2017 *Phys. Plasmas* **24** 112103
[55] Gansner E R and North S C 2000 *Softw. - Pract. Exp.* **30** 1203